ChemComm

Photoinduced ligand dissociation follows reverse energy gap law: nitrile photodissociation from low energy 3MLCT excited states

Journal:	*ChemComm*
Manuscript ID	CC-COM-12-2019-010095.R1
Article Type:	Communication

COMMUNICATION

Photoinduced ligand dissociation follows reverse energy gap law: nitrile photodissociation from low energy ^{3}MLCT excited states

Received 00th January 20xx,
Accepted 00th January 20xx

DOI: 10.1039/x0xx00000x

Lauren M. Loftus,[‡] Jeffrey J. Rack, [§] and Claudia Turro*[‡]

A series of Ru(II)-terpyridine complexes containing electron-donating bidentate ligands are able to effectively photodissociate nitrile ligands using red light. A spectroscopic investigation of these complexes reveal that they follow anti-energy gap law behavior, providing futher evidence that population of ^{3}LF excited states is not necessary for photoinduced nitrile dissociation.

Polypyridyl Ru(II) complexes have been used for a variety of applications due to their intense singlet metal-to-ligand charge transfer (MLCT) absorption in the visible region and long ^{3}MLCT excited state lifetimes.[1-5] For example, the well-known complex $[Ru(bpy)_3]^{2+}$ (bpy = 2,2′-bipyridine) absorbs strongly at ~450 nm and has a solvent-dependent ^{3}MLCT lifetime of 0.6 – 1 μs.[6,7] The ^{3}MLCT excited state of $[Ru(bpy)_3]^{2+}$ is also luminescent, with a phosphorescence quantum yield, Φ_{em}, of 0.042 in H_2O at 298 K.[8] However, this luminescence is highly temperature dependent, with Φ_{em} ranging from 0.38 at 77 K in EtOH to 0.0075 at 363 K in aqueous solution.[8,9] Additionally, $[Ru(bpy)_3]^{2+}$ undergoes ligand photosubstitution at 368 K in 0.1 M HCl to form $[Ru(bpy)_2Cl_2]$ upon irradiation with 436 nm light.[9] This temperature dependent behavior suggests that a non-emissive, dissociative excited state is present ~3800 cm^{-1} higher in energy than the emissive ^{3}MLCT state(s), and has been assigned as the triplet ligand field (^{3}LF) excited state(s).[9]

Although polypyridyl Ru(II) complexes derived from $[Ru(bpy)_3]^{2+}$ have been investigated extensively, those based on $[Ru(tpy)_2]^{2+}$ (tpy = 2,2′:6′,2″-terpyridine) are preferable for use in supramolecular systems due to their achiral D_{2d} symmetry.[10] However, the large deviation from octahedral geometry afforded by the bite angles of the tpy ligand, as compared to bpy, results in a decrease of the energy of the tpy–d_{z^2}(σ*) molecular orbital and, consequently, the energy gap between the ^{3}MLCT and ^{3}LF excited states, thus shortening the ^{3}MLCT lifetime of $[Ru(tpy)_2]^{2+}$ to 250 ps in H_2O and 124 ps in CH_3CN.[11,12] Increased population of the ^{3}LF excited state(s) is generally accepted as necessary for photoinduced ligand exchange, making Ru(II)-tpy complexes useful for light-initiated drug release in photochemotherapy (PCT).[13-17]

Previously, the photochemistry of a series of Ru(II) complexes, **1 – 11** (Fig. 1), was investigated by our group for photoinduced nitrile dissociation.[18] Using λ_{irr} = 450 nm, these complexes were found to exhibit a wide range of quantum yields of ligand dissociation, Φ_{450}, ranging from 0.0022(1) – 0.018(1) for the replacement of the CH_3CN ligand with a H_2O molecule, despite a lack of steric bulk around the metal center throughout the series.[18,19] Complexes **8 – 11** were also found to undergo efficient ligand dissociation using λ_{irr} = 650 nm. Density functional theory (DFT) calculations showed that within the series, the complexes with the larger quantum yield values, namely **8 – 11**, all possessed highest occupied molecular orbitals (HOMOs) in the ground state that were delocalized, as well as ^{3}MLCT excited states that were characterized by a low degree of electron density on the metal center.[18] These results were similar to previous findings from our group involving Ru(II) complexes with tetradentate ligands based on tris(2-pyridylmethyl)amine, and the greater quantum yields of **8 – 11** were thus attributed to decreased π-backbonding to the nitrile ligand in the ^{3}MLCT excited state.[18,20]

Given the unusual occurrence of increased ligand dissociation from ^{3}MLCT-type excited states, the present work details an investigation into the photophysical properties of **1 –**

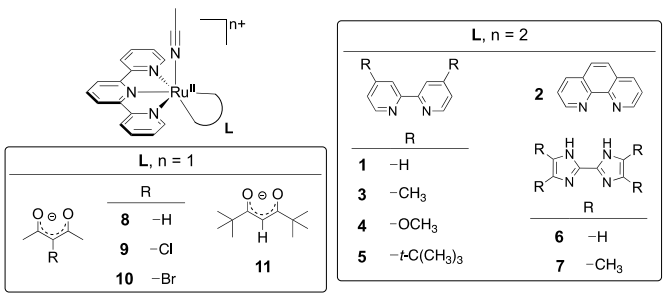

Fig. 1. Structures of complexes **1 – 11**; structures of **12** and **13** are shown in Fig. S1 (ESI).

[‡]*Department of Chemistry and Biochemistry, The Ohio State University, Columbus, Ohio 43210, USA. Email: turro.1@osu.edu*
[§]*Department of Chemistry and Chemical Biology, University of New Mexico, Albuquerque, NM 87131, USA. Email: jrack@unm.edu*
† Electronic Supplementary Information (ESI) available: experimental methods, molecular structures of **12** and **13**, complete fsTA and nsTA data for **1 – 13**, lifetimes for **1 – 11**. See DOI: 10.1039/x0xx00000x

11 utilizing femtosecond (fsTA) and nanosecond transient absorption spectroscopies (nsTA). Surprisingly, our findings indicate that the trend in the excited state lifetimes of **1** – **11** is opposite to that expected from the energy gap law, which dictates that the rate of nonradiative decay between two states should increase due to enhanced vibrational coupling as the energy gap between them decreases.[21] Complexes **8** – **11** possess both the lowest energy ^{3}MLCT excited states and the longest excited state lifetimes across the series. When considered together with the fact that **8** – **11** also exhibit the highest quantum yields of photoinduced nitrile dissociation, these results reinforce the hypothesis that population of the ^{3}LF excited states is not necessary to achieve efficient dissociation of nitrile-based ligands.

The ground state electronic absorption spectra of **1** – **11** in acetone are shown in Fig. S2 (ESI), which exhibit a ^{1}MLCT absorption in the visible region (ε = 5400 – 11,000 M^{-1} cm^{-1}) corresponding predominately to a Ru(dπ) $\rightarrow$ tpy(π^*) transition. In **1** – **5**, this band also contains some contribution of Ru(dπ) $\rightarrow$ diimine(π^*) character. The π-donor character of the electron-rich acetylacetonate-based ligands present in **8** – **11** destabilize the Ru(dπ) orbitals, making the metal center significantly easier to oxidize and shifting the energy of the ^{1}MLCT absorption maximum to lower energy by ~3300 cm^{-1} as compared to **1**.[19]

Excitation of **1** in CH_3CN into the low energy side of the ^{1}MLCT transition (λ_{ex} = 505 nm) is expected to lead to selective population of the Ru(dπ) $\rightarrow$ tpy(π^*) ^{1}MLCT excited state, resulting in the fsTA spectra shown in Fig. 2. A ground state bleach is observed centered at 450 nm, and positive signal is observed at ~350 – 390 nm and 530 – 650 nm associated with the reduced tpy$^-$($\pi\rightarrow\pi^*$) and bpy(π) $\rightarrow$ Ru^{3+}(dπ) ligand-to-metal charge transfer (^{3}LMCT) transitions, respectively. The observation of both of these excited state absorptions is indicative of an excited state containing both a reduced ligand and an oxidized metal center, and is thus consistent with population of the ^{3}MLCT excited state. The excited state absorption of **1** from 360 – 390 nm can be fitted to a biexponential function with lifetimes, τ, of 6(1) ps (40%) and 75(11) ps (60%) (Fig. S3, ESI), similar to the kinetics observed for the ^{3}LMCT excited state absorption. In contrast, the kinetics of the ground state bleach region are monoexponential with τ = 75(8) ps (Fig. S3 and Table S1, ESI). Complexes **2** – **5** also contain diimine-based bidentate ligands and exhibit similar fsTA spectra with lifetimes that range from 4 – 11 ps for the short component lifetime, as well as monoexponential decay of the bleach signals (Fig. S4 – S7, Table S1, ESI).

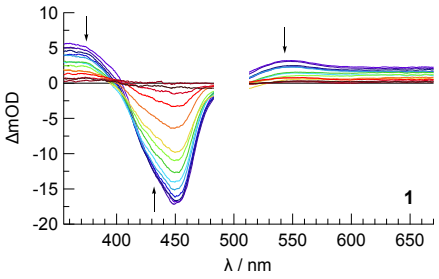

Fig. 2. fsTA spectra of **1** in CH_3CN collected at 1, 2, 5, 8, 11, 21, 29, 39, 54, 73, 116, 184, 398 and 2928 ps after the laser pulse (λ_{ex} = 505 nm, baseline collected at -20 ps, fwhm ~85 fs).

There are two likely possibilities as to the nature of the fast time component observed in the excited state absorption features of **1** – **5**. The first of these is simply vibrational cooling within the ^{3}MLCT manifold, which tends to occur on a similar timescale. However, given that vibrational relaxation tends to manifest spectroscopically as a narrowing in the peak shape of the excited state absorption feature coupled with an increase and slight blueshift of the peak signal, and the low excitation energies used, vibrational relaxation is not consistent with the observed fsTA of **1** – **5** at early times.[22-24] The second possibility is that the fast component is due to an equilibrium between the ^{3}MLCT and ^{3}LF excited states of **1** – **5**, as has been observed by Hewitt and co-workers in $[Ru(tpy)_2]^{2+}$ on similar timescales.[11] Their observation of this equilibrium leading to an overall decrease in signal in the excited state absorption region is more consistent with the spectral features observed for **1** – **5**. The exact nature of this fast component remains under investigation, as the presence of a ^{3}MLCT – ^{3}LF excited state equilibrium in the complexes with lower ligand exchange quantum yields could have interesting implications regarding the mechanism of ligand photodissociation.

Low energy excitation of **6** and **7** in CH_3CN (λ_{ex} = 550 and 565 nm, respectively) result in fsTA spectra (Figs. S8 and S9, ESI) that are qualitatively similar to those observed for **1** – **5** and characteristic of population of a ^{3}MLCT excited state. Both **6** and **7** show reduced tpy$^-$($\pi\rightarrow\pi^*$) excited state signal from ~350 – 420 nm with slightly red-shifted maxima relative to the diimine complexes, attributed to the red-shifted ground state absorption of **6** and **7** (Fig. S2, ESI). Single wavelength kinetics in this region for **6** (Table S1, ESI) show a slow rise in absorption that was fit biexponentially with τ_1 fixed at the instrument response function (85 fs), which resulted in τ_2 = 20(8) ps, and the decay was fit to a monoexponential function with τ = 650(30) ps. The recovery of the ground state bleach of **6** from 420 – 500 nm was fit to a biexponential decay, with τ_1 fixed at 20 ps (3%) corresponding to the slow rise of the excited state absorption (due to the spectral overlap of the two features), which resulted in τ_2 = 590(30) ps (97%). Due to the long excited state lifetime of **6**, a small amount of residual signal remains at the end of the fsTA experiment (~3 ns).

The positive signal of the absorption of the reduced tpy in the excited state of **7** exhibits a monoexponential decay with τ = 2.7(6) ns, and the ground state bleach from 420 – 500 nm returns to the baseline monoexponentially with τ = 1.7(2) ns (Table S1, ESI). A small amount of excited state absorption is also present in **7** from 500 – 550 nm with greater intensity than observed in **6**, which is also attributed to a ^{3}LMCT $Me_4bim \rightarrow Ru^{3+}$(d$\pi$) transition in the ^{3}MLCT excited state. The higher intensity in **7** as compared to **6** can be explained by the greater electron-donating character of the bidentate ligand in the former. Unfortunately, the low signal in this region precluded the measurement of reliable kinetic information for **6** and **7**.

Excitation into the ^{1}MLCT transition of **8** in CH_3CN (λ_{ex} = 585 nm) yields the fsTA spectra shown in Fig. 3a. Similar to **1** – **7**, an excited state absorption is observed in **8** from 360 – 440 nm,

arising from a $\pi \rightarrow \pi^*$ transition within the reduced tpy ligand, indicating population of the ^{3}MLCT excited state. A ground state bleach is also observed in **8** from 440 – 550 nm. Surprisingly, there is relatively little decay of these signals observed within the timescale of the ultrafast experiment (~3 ns). Transient absorption spectra of **8** on the nanosecond timescale (λ_{ex} = 580 nm, Fig. 3b) in CH_3CN show similar features to those observed in the ultrafast experiment, indicating continued population of the ^{3}MLCT state. Single wavelength kinetic traces of both the excited state absorption and ground state bleach can be fit to a single decay component with τ = 7.2(3) and 6.9(5) ns, respectively (Fig. S10, Table S1, ESI). Complexes **9** – **11** behave similarly, with spectral features indicative of ^{3}MLCT excited states that persist into the nanosecond timescale, with lifetimes ranging from 3.7(6) to 7.8(3) ns (Fig. S11 – S13, Table S1, ESI).

Complex **8** was also investigated using ultrafast time-resolved infrared spectroscopy (TRIR), as the acetylacetonato (acac) ligand provides strong IR markers. Excitation of **8** in CD_3CN with 518 nm light shows several excited state vibrations from 1300 – 1600 cm^{-1} (Fig. 3c). Three intense acac-based vibrations are present in the ground state IR spectrum (dotted line, Fig. 3c) at 1405, 1517, and 1571 cm^{-1} corresponding to $\delta(CH_3)$ and ν(C=O), ν(C=C) and δ(C=CH), and predominately ν(C=O) modes, respectively.[25,26] In the excited state, the bleach of these ground state IR absorptions indicates the removal of electron density from a mixed Ru/acac HOMO, in agreement with our previous DFT calculations.[18] These vibrations shift to lower energies in the excited state, appearing at ~1350, 1492 and 1525 cm^{-1}, respectively. These shifts are again indicative of a ^{3}MLCT-based excited state, as a ^{3}LF excited state would be localized on the metal center and should not significantly perturb the electron density of the ligands, leading to a smaller energy shift in the excited state as observed in TRIR spectra of $Cr(acac)_3$ and $Fe(acac)_3$.[27,28] At early times, the excited state vibration centered at 1492 cm^{-1} narrows and increases in intensity with τ ~6 ps, characteristic of vibrational cooling in the excited state that is likely a result of excitation at the ^{1}MLCT maximum in the TRIR experiment instead of the red edge. Overall, however, the significant shifts in energy of these ligand-based vibrations remain throughout the experiment (~3 ns), in agreement with the assignment of a long-lived ^{3}MLCT excited state with significant contribution from the acac ligand.

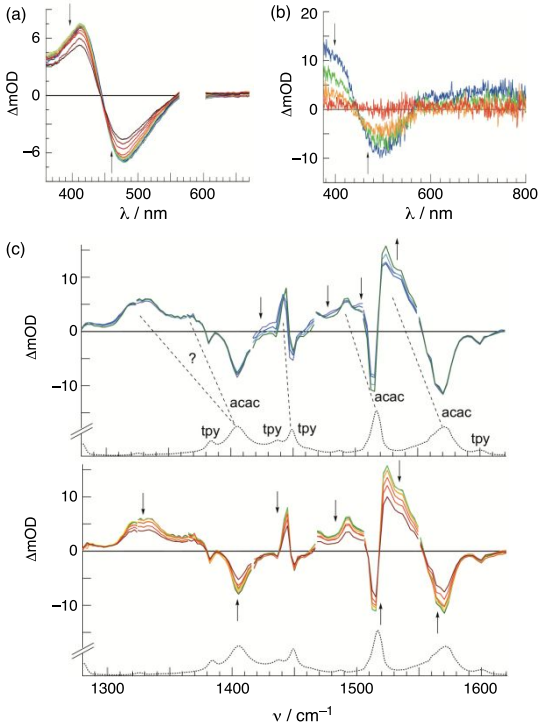

Fig. 3. (a) fsTA of **8** in CH_3CN collected at 1, 3, 6, 9, 24, 46, 63, 99, 250, 463, 630, 999, 2154 and 2928 ps after the laser pulse (λ_{ex} = 585 nm, fwhm ~85 fs), (b) nsTA of **8** in CH_3CN collected at 0, 2, 6 and 20 ns after the laser pulse (λ_{ex} = 580 nm, fwhm ~12 ns), and (c) TRIR spectra of **8** in CD_3CN collected at 1.5, 4.3, 14 and 29 ps after the laser pulse (top) and 29, 67, 179, 359, 722, 1453 and 2716 ps after the laser pulse (bottom, λ_{ex} = 518 nm, fwhm ~300 fs); the ground state FTIR spectrum of **8** in CD_3CN is shown as a dotted line.

When the excited state lifetimes of **1** – **11** are considered together, it is apparent that the complexes with the lowest energy ^{3}MLCT excited states, namely **8** – **11**, also possess longer excited state lifetimes (Fig. 4a), in disagreement with the energy gap law. Similar trends have been observed in other tpy-based Ru(II) complexes, as selective stabilization of the ^{3}MLCT excited state results in an increased energy gap between the ^{3}MLCT and ^{3}LF states, thus reducing deactivation of the former through the latter.[10,29,30] Surprisingly, of the complexes in this series, those with the longest ^{3}MLCT lifetimes, **8** – **11**, also exhibit the largest quantum yields of ligand dissociation (Fig. 4b).

While one could argue that the increased quantum yields observed in **8** – **11** are due to the simultaneous stabilization of the ^{3}LF excited state(s) afforded by the weaker ligand field strength of the acac-based ligands, as has been observed in other Ru(II) complexes with electron-donating ligands, the experimentally observed increase in their excited state lifetimes (Fig. 4b) is contrary to this notion.[31-33] It is expected that the presence of more accessible ^{3}LF states would lead to a decrease in the observed ^{3}MLCT excited state lifetime, similar to the shorter lifetime of $[Ru(tpy)_2]^{2+}$ compared to $[Ru(bpy)_3]^{2+}$.[6,30,34]

The excited state properties of the related complexes $[Ru(dqpy)(phen)(CH_3CN)]^{2+}$, **12**, and $[Ru(dqpy)(acac)(CH_3CN)]^{+}$,

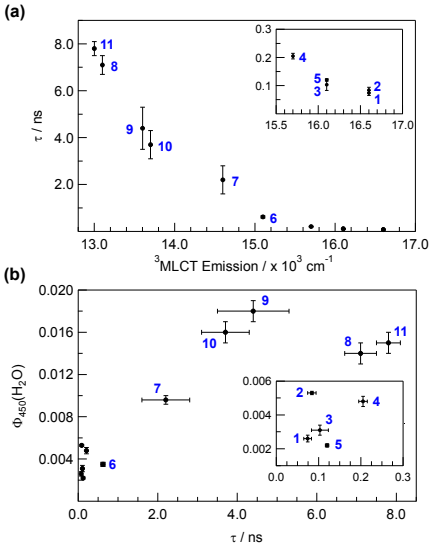

Fig. 4. (a) Relationship between the excited state lifetime of **1** – **11** and the ^{3}MLCT emission maximum at 77 K in CH_3CN, and (b) between the quantum yield of ligand dissociation in H_2O, Φ_{450}, and the excited state lifetime of **1** – **11**.

13, (Fig. S1, ESI; dqpy = 2,6-di(quinoline-2-yl)pyridine, phen = 1,10-phenanthroline) were also investigated. The dqpy ligand is more easily reduced than tpy, thus **12** and **13** exhibit lower energy ^{3}MLCT excited states as compared to the corresponding tpy complexes **2** and **8**, respectively.[35] Transient absorption spectra of **12** and **13** in CH_3CN exhibit similar trends (Figs. S14 and S15, ESI), with ^{3}MLCT excited state lifetimes of ~400 ps and 14(1) ns, respectively, compared to 80(10) ps and 7.1(4) ns for **2** and **8**. Importantly, the dqpy complexes exhibit quantum yields of ligand dissociation with λ_{irr} = 600 nm in H_2O that are nearly identical to those of **2** and **8**, with Φ_{600} = 0.0050(2) and 0.010(1) for **12** and **13**, respectively, as compared to Φ_{450} = 0.0053(1) and 0.014(1) for **2** and **8**.[18,35] This result demonstrates that lowering the energy of the ^{3}MLCT excited state does not impact the quantum yield of nitrile photodissociation, even when the identity of the bidentate ligand is held constant.

In the present work, we have spectroscopically shown that complexes **1** – **13** exhibit increasing ^{3}MLCT lifetimes as the energy of the ^{3}MLCT excited state is stabilized. This anti-energy gap law behaviour suggests that the complexes with the lowest energy ^{3}MLCT excited states are less able to efficiently populate the dissociative ^{3}LF state(s), thus extending their lifetimes. Surprisingly, the complexes that have the longest ^{3}MLCT excited state lifetimes, namely **8** – **11** and **13**, also show the greatest quantum yields of nitrile ligand dissociation. Together, these results suggest that population of the ^{3}LF state(s) is not necessary for photodissociation of nitrile ligands, and demonstrate that photoinduced nitrile dissociation can occur in relatively unstrained Ru(II) complexes with low energy ^{3}MLCT excited states due to differences in π-backbonding between the ground state and ^{3}MLCT excited states.[18] These findings represent a paradigm shift in the design of Ru(II)-based PCT drugs, and open new possibilities for complexes that both undergo efficient photoinduced ligand dissociation *and* absorb red light in the photodynamic therapy window. Current work in our lab to investigate the temperature-dependent properties of these complexes is ongoing.

The authors wish to thank the National Science Foundation (CHE-1800395) for their generous support of this work, as well as the Center for Chemical and Biophysical Dynamics (CCBD) and the Ohio Supercomputer Center for use of their facilities. JJR acknowledges the National Science Foundation for financial support of this work (CHE-1856492 and CHE-1602240).

Conflicts of interest

There are no conflicts to declare.

Notes and references

1. V. Balzani, G. Bergamini and P. Ceroni, *Coord. Chem. Rev.*, 2008, **252**, 2456-2469.
2. P. Ceroni, A. Credi and M. Venturi, *Chem. Soc. Rev.*, 2014, **43**, 4068-4083.
3. L. Hammarström, *Acc. Chem. Res.*, 2015, **48**, 840-850.
4. K. Kalyanasundaram and M. Graetzel, *Curr. Opin. Biotechnol.*, 2010, **21**, 298-310.
5. D. W. Thompson, A. Ito and T. J. Meyer, *Pure Appl. Chem.*, 2013, **85**, 1257-1305.
6. A. Juris, V. Balzani, F. Barigelletti, S. Campagna, P. Belser and A. von Zelewsky, *Coord. Chem. Rev.*, 1988, **84**, 85-277.
7. Y. Kaizu, H. Ohta, K. Kobayashi, H. Kobayashi, K. Takuma and T. Matsuo, *J. Photochem.*, 1985, **30**, 93-103.
8. K. Kalyanasundaram, *Coord. Chem. Rev.*, 1982, **46**, 159-244.
9. J. Van Houten and R. J. Watts, *J. Am. Chem. Soc.*, 1976, **98**, 4853-4858.
10. E. A. Medlycott and G. S. Hanan, *Coord. Chem. Rev.*, 2006, **250**, 1763-1782.
11. J. T. Hewitt, P. J. Vallett and N. H. Damrauer, *J. Phys. Chem. A*, 2012, **116**, 11536-11547.
12. J. R. Winkler, T. L. Netzel, C. Creutz and N. Sutin, *J. Am. Chem. Soc.*, 1987, **109**, 2381-2392.
13. K. Arora, M. Herroon, M. H. Al-Afyouni, N. P. Toupin, T. N. Rohrabaugh, L. M. Loftus, I. Podgorski, C. Turro and J. J. Kodanko, *J. Am. Chem. Soc.*, 2018, **140**, 14367-14380.
14. J. D. Knoll, B. A. Albani, C. B. Durr and C. Turro, *J. Phys. Chem. A*, 2014, **118**, 10603-10610.
15. L. N. Lameijer, D. Ernst, S. L. Hopkins, M. S. Meijer, S. H. C. Askes, S. E. Le Dévédec and S. Bonnet, *Angew. Chem., Int. Ed.*, 2017, **56**, 11549-11553.
16. C. R. Hecker, P. E. Fanwick and D. R. McMillin, *Inorg. Chem.*, 1991, **30**, 659-666.
17. M. Frasconi, Z. Liu, J. Lei, Y. Wu, E. Strekalova, D. Malin, M. W. Ambrogio, X. Chen, Y. Y. Botros, V. L. Cryns, J.-P. Sauvage and J. F. Stoddart, *J. Am. Chem. Soc.*, 2013, **135**, 11603-11613.
18. L. M. Loftus, K. F. Al-Afyouni, T. N. Rohrabaugh Jr., J. C. Gallucci, C. E. Moore, J. J. Rack and C. Turro, *J. Phys. Chem. C*, 2019, **123**, 10291-10299.
19. L. M. Loftus, K. F. Al-Afyouni and C. Turro, *Chem. - Eur. J.*, 2018, **24**, 11550-11553.
20. L. M. Loftus, A. Li, K. L. Fillman, P. D. Martin, J. J. Kodanko and C. Turro, *J. Am. Chem. Soc.*, 2017, **139**, 18295-18306.
21. E. M. Kober, J. V. Caspar, R. S. Lumpkin and T. J. Meyer, *J. Phys. Chem.*, 1986, **90**, 3722-3734.
22. G. B. Shaw, D. J. Styers-Barnett, E. Z. Gannon, J. C. Granger and J. M. Papanikolas, *J. Phys. Chem. A*, 2004, **108**, 4998-5006.
23. S. Wallin, J. Davidsson, J. Modin and L. Hammarström, *J. Phys. Chem. A*, 2005, **109**, 4697-4704.
24. S. Wallin, J. Davidsson, J. Modin and L. Hammarström, *J. Phys. Chem. A*, 2005, **109**, 9378.
25. M. Vakili, S. F. Tayyari, M. Hakimi-Tabar, A.-R. Nekoei and S. Kadkhodaei, *J. Mol. Struct.*, 2014, **1058**, 308-317.
26. I. Diaz-Acosta, J. Baker, W. Cordes and P. Pulay, *J. Phys. Chem. A*, 2001, **105**, 238-244.
27. E. M. S. Maçôas, R. Kananavicius, P. Myllyperkiö, M. Pettersson and H. Kunttu, *J. Am. Chem. Soc.*, 2007, **129**, 8934-8935.
28. E. M. S. Maçôas, R. Kananavicius, P. Myllyperkiö, M. Pettersson and H. Kunttu, *J. Phys. Chem. A*, 2007, **111**, 2054-2061.
29. E. A. Medlycott and G. S. Hanan, *Chem. Soc. Rev.*, 2005, **34**, 133-142.
30. C. R. Hecker, A. K. I. Gushurst and D. R. McMillin, *Inorg. Chem.*, 1991, **30**, 538-541.
31. G. Malouf and P. C. Ford, *J. Am. Chem. Soc.*, 1974, **96**, 601-603.
32. G. Malouf and P. C. Ford, *J. Am. Chem. Soc.*, 1977, **99**, 7213-7221.
33. E. Tfouni and P. C. Ford, *Inorg. Chem.*, 1980, **19**, 72-76.
34. J. R. Kirchhoff, D. R. McMillin, P. A. Marnot and J. P. Sauvage, *J. Am. Chem. Soc.*, 1985, **107**, 1138-1141.
35. M. H. Al-Afyouni, T. N. Rohrabaugh Jr, K. F. Al-Afyouni and C. Turro, *Chem. Sci.*, 2018, **9**, 6711-6720.

Table of Contents Figure

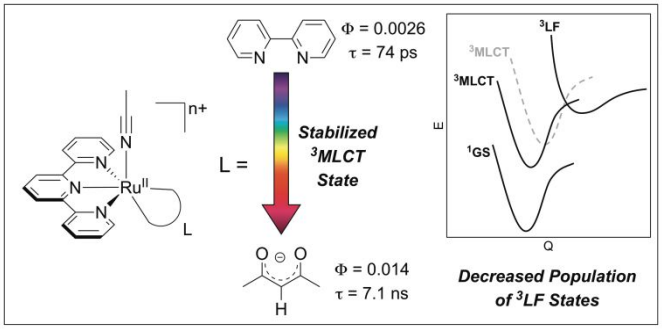

Transient absorption spectroscopy is used to show that stabilization of the ^{3}MLCT excited state in a series of Ru(II) complexes leads to decreased population of the ^{3}LF state, but does not reduce the efficiency of photoinduced nitrile dissociation.